Characterization of *Notch*-class gene expression in segmentation stem cells and segment founder cells in *Helobdella robusta* (*Lophotrochozoa; Annelida; Clitellata; Hirudinida; Glossiphoniidae*)

Ajna S. Rivera, Foster C. Gonsalves, Mi Hye Song[1], Brian J. Norris[2], and David A. Weisblat*

Department of Molecular and Cell Biology, 385 LSA University of California, Berkeley, CA 94720-3200, USA

*Author for correspondence (email: weisblat@uclink.berkeley.edu)

[1]Present address: Laboratory of Biochemistry and Genetics, NIDDK/NIH, Building 8, Room 2A07, Bethesda, MD 20892, USA.

[2]Present address: Department of Biological Sciences, California State University, San Marcos, CA 92096, USA.

SUMMARY To understand the evolution of segmentation, we must compare segmentation in all three major groups of eusegmented animals: vertebrates, arthropods, and annelids. The leech *Helobdella robusta* is an experimentally tractable annelid representative, which makes segments in anteroposterior progression from a posterior growth zone consisting of 10 identified stem cells. In vertebrates and some arthropods, Notch signaling is required for normal segmentation and functions via regulation of *hes*-class genes. We have previously characterized the expression of an *hes*-class gene (*Hro-hes*) during segmentation in *Helobdella*, and here, we characterize the expression of an *H. robusta notch* homolog (*Hro-notch*) during this process. We find that *Hro-notch* is transcribed in the segmental founder cells (blast cells) and their stem-cell precursors (teloblasts), as well as in other nonsegmental tissues. The mesodermal and ectodermal lineages show clear differences in the levels of *Hro-notch* expression. Finally, *Hro-notch* is shown to be inherited by newly born segmental founder cells as well as transcribed by them before their first cell division.

INTRODUCTION

Annelids, arthropods, and vertebrates are widely accepted as meeting even the most stringent definitions of segmentation, also known as "eusegmentation." In species of these taxa, two or more tissues or organs systems (nervous, muscular, excretory, circulatory, and/or integumental) are organized metamerically along the anteroposterior (A–P) axis of the animal; metamers of different systems have the same repeat length; and new metamers are added sequentially to the posterior end of the chain (Willmer 1990). But whether segmentation represents convergent evolution or descent from a common segmented ancestor is still a question of interest and debate (e.g., Budd 2001; Scholtz 2002; Balavoine and Adoutte 2003). Phylogenetic evidence favors convergence between deuterostomes (vertebrates) and protostomes (annelids and arthropods) (Davis and Patel 1999). However, recent studies of molecular mechanisms have revealed intriguing similarities in segmentation between some arthropods and vertebrates.

In vertebrates, segmental mesoderm (somites) arise as transiently epithelialized groups of cells that bud off from the anterior end of the presomitic mesoderm (PSM). This process has been explained by a "clock-and-wave front" model (Cooke and Zeeman 1976), and there is now good molecular

evidence for this model (Lewis 2003). The "clock" corresponds to a biochemical oscillator in which the auto-inhibitory expression of *hairy/Enhancer of split-* (*hes*) class genes (Palmeirim et al. 1997) is driven and/or synchronized by oscillating signals from the Notch/Delta pathway (Evrard et al. 1998; Morales et al. 2002; Aulehla et al. 2003) whereas the "wave front" corresponds to an anteriorly decreasing gradient of fibroblast growth factor (FGF)-8 that originates from the posterior of the PSM (Dubrulle and Pourquie 2004).

The eponymous *hairy* gene was identified as a pair rule gene in the segmentation cascade of *Drosophila melanogaster* (Holmgren 1984). *Drosophila* segments form simultaneously from a syncytial blastoderm in a process that differs dramatically from vertebrate somitogenesis. However, the *Drosophila* condition is evolutionarily derived within the arthropods (Peel 2004). Thus, the initial discovery that genes related to *hairy* are involved in vertebrate somitogenesis led to speculation of a segmented bilaterian ancestor (Kimmel 1996; Muller et al. 1996). More recently, additional support for this view has been provided from studies of a spider, *Cupiennius salei,* which segments sequentially from a posterior differentiation zone, which is at least analogous to the situation in vertebrates. In situ hybridization studies reveal variable patterns of expression for genes including *Csa-hairy* and *Csa-delta*, con-

sistent with the operation of a biochemical oscillator similar to that in vertebrates. Moreover, when the Notch signaling pathway was disrupted in *C. salei*, the normal pattern of segmentation was disrupted (Stollewerk et al. 2003; Schoppmeier and Damen 2005).

Although recent molecular phylogenies suggest that *Articulata* is paraphyletic (Aguinaldo et al. 1997), they concur with traditional phylogenies in uniting the various annelid taxa with arthropods within *Protostomia* to the exclusion of vertebrates. Thus, if the urbilaterian was segmented, and assuming uniform average rates of divergence, it might be predicted that segmentation processes in annelids and arthropods would show greater similarity to each other than to those in vertebrates. Among annelids, the glossiphoniid leech *Helobdella robusta* has been relatively well studied in terms of experimental embryology. Leeches are morphologically derived with respect to other annelids, given their anterior and posterior suckers and their loss of chaetae. But their early development is well conserved, at least with respect to clitellate annelids, as is best documented by comparisons of tubificid oligochaetes and glossiphoniid leeches (e.g., Goto et al. 1999). The experimental advantages of *Helobdella* makes it a useful reference for comparing annelids with other taxa.

Like other clitellate annelids, *H. robusta* is hermaphroditic. Fertilization is internal but the zygote (approximately 400 μm in diameter) arrests in meiosis I until deposition. Between polar body formation and first cleavage, domains of yolk-deficient cytoplasm (teloplasm) form at the animal and vegetal poles (Fig. 1; Fernandez 1980). In a modified version of spiral cleavage lasting approximately 30 h after zygote deposition (AZD), teloplasm is partitioned first into macromere D′ and then into five bilateral pairs of large segmentation stem cells (M, N, O/P, O/P, and Q teloblasts). Cleavage also generates a set of 25 small cells called micromeres (Bissen and Weisblat 1989).

Each teloblast undergoes iterated and highly asymmetric divisions, generating segment founder cells (primary blast cells) in coherent columns (bandlets). The birth order of the blast cells is maintained within each bandlet, so the first-born blast cells lie distal to the parent teloblast and contribute to more anterior segments. The five bandlets on each side merge into a parallel array called a germinal band, which lies at the surface of the embryo (Fig. 1), covered by a squamous epithelium derived from micromeres. During gastrulation, the left and right germinal bands move over the surface of the embryo and gradually coalesce from anterior to posterior into the germinal plate, from which segments arise. The movements of the germinal bands are accompanied by an epibolic expansion of the micromere-derived epithelium (micromere cap). There is one pair of mesodermal (M) teloblasts and four pairs of ectodermal (N, O/P, O/P, and Q) teloblasts, each of which contributes a distinct set of several dozen segmentally iterated progeny (M, N, O, P, and Q kinship groups) to the
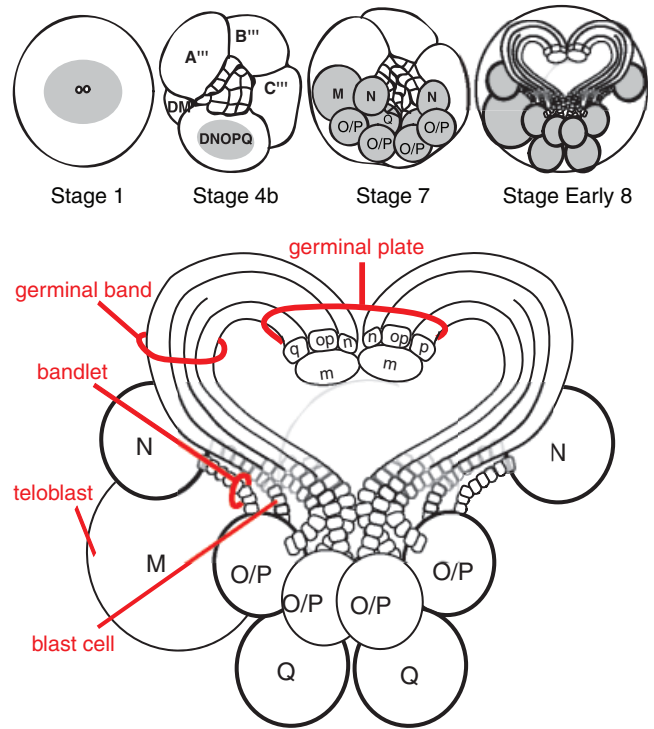
Fig. 1. Formation and function of the teloblastic growth zone in *Helobdella*. The upper panels show key stages in early development. Stage 1: in the zygote, cytoplasmic rearrangements generate animal and vegetal domains of yolk-free cytoplasm (teloplasm, shading). Stage 4b: during the early cleavages, teloplasm (shading) is segregated to the D quadrant and hence to proteloblasts DM and DNOPQ, precursors of segmental mesoderm and ectoderm, respectively. Stage 7: during later cleavage the proteloblasts give rise to bilateral pairs of M, N, O/P, O/P, and Q teloblasts (gray), along with additional micromeres. (Not all teloblasts are visible in this view.) Stage early 8: teloblasts undergo iterated, unequal divisions to form columns (bandlets) of blast cells. The five bandlets on each side of the embryo merge in parallel to form left and right germinal bands. The germinal bands move over the surface of the embryo, coalescing along the ventral mid-line in anteroposterior (A–P) progression and forming the germinal plate, from which definitive segments arise. (A micromere-derived epithelium that covers the germinal bands and the area between them is not shown.) The bottom drawing shows a more detailed view of the teloblasts and their derivatives at stage 8.

definitive segments via the stereotyped divisions of the blast cells (Weisblat and Shankland 1985; Braun and Stent 1989; Zhang and Weisblat 2005).

Thus, segmentation in leech is strictly linked to the cell division patterns of the teloblasts and their blast cell progeny. So if leech embryos have a biochemical oscillator linked to segmentation as in vertebrates, it should also be linked to the cell cycle. To extend the analysis of segmentation in *H. robusta* to the molecular level, and in particular to assess the extent to which it resembles segmentation in arthropods and vertebrates, we have previously characterized the expression

of an *hes*-class gene, *Hro-hes* (Song et al. 2004). The findings of this work are consistent with the idea that *Hro-hes* plays a role in segmentation; *Hro-hes* is expressed throughout cleavage, but peaks during the period when teloblasts are generating blast cells. Moreover, the localization of *Hro-hes* transcript and HRO-HES protein shows a strong cell cycle dependence in the early blastomeres, teloblasts, and blast cells. HRO-HES protein is readily observed in association with the nucleus of cells during interphase, but is much reduced in the nuclear region during mitosis. In contrast, *Hro-hes* transcripts show a punctate distribution in the region of the nucleus of cells in mitosis. This punctate staining is blocked by transcription inhibitors, and RT-PCR of carefully staged zygotes shows unambiguously that *Hro-hes* is transcribed during mitosis at least during the first zygotic mitosis, something that has not been reported for an *hes* homolog in any other system.

To complement the ongoing analysis of *Hro-hes*, we have begun to look for the participation of *notch*-class genes in annelid segmentation. Here, we report having isolated the 3′ portion of *Hro-notch*, a *notch*-class gene from *H. robusta*, encoding the putative transmembrane domain and the intracellular domain (HRO-NICD) and the complete 3′ untranslated region (UTR). We have also characterized the expression of *Hro-notch* by in situ hybridization, focusing here on segmentation. We find differences in the expression of *Hro-notch* between teloblasts and blast cells and between the ectodermal and mesodermal lineages, including cell cycle-dependent aspects of its expression.

MATERIALS AND METHODS

Hro-Notch cloning
Degenerate primers Notch3S: GGGTCGACGRTCCATRTGRT CNGTDAT and Notch5S: GAGAGCTCCAYTGGGCNGCNG CNGT were used to amplify a fragment of *Hro-Notch* from a complementary DNA (cDNA) library made commercially (Stratagene, La Jolla, CA, USA) from stage 7 to 10 cDNA. Subsequently a λ DASH II genomic library made from *H. robusta* was plated onto nylon membranes and screened for *Hro-notch* using an 180-bp fragment from the original sequence as probe. Primers used for amplifying this fragment were NPr2F1: CCATCGCGACGG-GGGTG and NPr2R1: ATTTCGAGAGAGGGGACGCAGC. The probe was labeled with ^{32}P labeled dCTP using a Klenow-based Prime-It II kit from Stratagene (Cat # 300,385). Conditions for the labeling reaction were as recommended by the manufacturer. Hybridization was carried out at 37°C for 36 h. The filters were then washed in 2 × SSC, 0.1% sodium dodecyl sulfate at room temperature for 15 min followed by two washes at 55°C for 30 min. Subsequently filters were exposed to X-ray film at − 80°C for 16 h. Two lifts from each plate were screened; the total number of plaques screened was approximately 180,000. The screen yielded a total of eight positive plaques of which N4A1 was sequenced. Based on the genomic sequence information, the following gene

specific primers were used to amplify a 2510 bp of the intracellular domain of *Hro-notch* (*Hro-nicd*) from 199 stages 4c-8 embryos: NICDF2: TGG TGGCAACGCCTGACTACTTTC and NI-CDR4: AATCTGGC GAGGGTGTAGGGTAC.

The following cycling parameters: 95°C for 1 min, 57°C for 1 min, 72°C for 2 min for 30 cycles. Sequence analysis was performed using Sequencher 4.2 (Gene Codes Corp., Ann Arbor, MI, USA) and BLAST (NCBI).

Semi-quantitative RT-PCR
Fifteen embryos from each stage were collected and homogenized in RNA-wiz (Ambion Inc., Austin, TX, USA). Total RNA was prepared as recommended by manufacturer. To analyze relative levels of Notch mRNA expression we amplified a fragment of Notch using either of the following two pairs of primers, N11: TTATTGGAAGCCG GTGGCGATCCG and N14: GGGTGC-ATCCGACTCGTTGTTGGG or NRTF1: AACAAACCCTTC-CTACCTGGC and NRTR1: ATCCAGATCGGTCGAACCT GT. Both primer pairs gave comparable results. The cycling parameters used were 95°C for 20 sec, 58°C for 30 sec, and 72°C for 1 min. To normalize for differences in RNA extraction efficiency between individual samples, we amplified an approximately 450-bp band from 18S rRNA-derived-cDNA using commercially available primer pairs (Ambion Inc.). The cycles used for this purpose were 95°C for 1 min, 58°C for 1 min, and 72°C for 30 sec. Samples from the reactions were collected in the exponential phase of amplification and resolved on a 1.5% agarose gel. Band intensity was computed using the Alpha-Imager gel-imaging system; ratios for *Hro-notch* amplicon intensity to that of the 18S amplicon were determined and plotted to reveal the mRNA expression profile.

Embryos
Embryos of the strain of *H. robusta* collected in Sacramento, California (Shankland et al. 1992) were obtained from a laboratory colony and cultured at 23°C in HL medium (Blair and Weisblat 1984). The embryonic staging system and cell nomenclature are as reviewed elsewhere (Huang et al. 2001). To block RNA synthesis, embryos were bathed in actinomycin-D mannitol (Sigma, St. Louis, MO, USA), 100–500 g/ml and 0.5% dimethyl sulfoxide in HL saline for 4–24 h at room temperature or pressure injected with 75 μg/ml α-amanitin (Sigma), as described previously (Bissen and Weisblat 1991). Lineage tracer injections and counterstaining were carried out as described previously (e.g., Song et al. 2004).

In situ hybridization
Digoxygenin (Dig-11-UTP, Roche, Indianapolis, IN, USA)-labeled riboprobes were made in vitro from linearized plasmid pNICDcl.11, using MEGAscript kit (Ambion Inc.). T7 or SP6 RNA polymerase (Ambion Inc.) was used to prepare all probes. The primers used were:

N14: GGGTGCATCCGACTCGTTGTTGGG and
N11: TTATTGGAAGCCGGTGGCGATCCG or
Nseq1R: ATCGCCACCGGCTTCCAATAA and
NicdF2: TGGTGGCAACGCCTGACTACTTTC

for the short and longer probes, respectively.

Embryos were fixed in 4% formaldehyde, 0.75 × phosphate-buffered saline (PBS, diluted from 10 × diethyl pyrocarbonate-treated PBS stock, pH 7.4), and 0.1% Tween (Bio-Rad, Hercules, CA, USA) for 1 h at room temperature. Fixed embryos were rinsed with 1 × PBTw (PBS, 0.1% Tween-20) then dehydrated in methanol and stored at 4°C for 3 days to 2 weeks. Embryos were then rehydrated with PBTw and devitellinized. Embryos were then incubated in hybridization solution (HYB, 50% formamide, 5 × SSC, 50 µg/ml heparin, 500 µg/ml tRNA, 0.1% Tween-20, citric acid to pH 6.0) overnight at 66°C with rocking. HYB was replaced with fresh HYB containing riboprobes and hybridized at 66°C for 28–40 h. Embryos were washed with pre-warmed HYB:SSC (2:1, 1:1, 1:2) for 5 min each, and then twice with 0.2 × SSC and 0.1 × SSC for 20 min at 66°C. Embryos were then moved to room temperature and washed for five minutes in solutions of 0.1 × SSC:PBTw (2:1, 1:1, 1:2) and then in PBTw. Embryos were then incubated in blocking solution (0.1% PBTw, 2% sheep serum (Sigma), 2 mg/ml bovine serum albumin) for 2 h at room temperature and further incubated in blocking solution containing anti-digoxygenin alkaline phosphatase-conjugated polyclonal Fab fragments (1:5000, Roche) at 4°C overnight followed by 4 h at room temperature. Embryos were rinsed with frequent changes of 0.1% PBTw for 3 h at room temperature, followed by three brief rinses with alkaline phosphatase buffer (AP buffer; 100-mM Tris-HCl, pH 9.5, 100-mM NaCl, 50-mM MgCl$_2$, 0.1% Tween 20). Embryos were then incubated in AP buffer containing 4-nitro blue tetrazolium chloride/5-bromo-4-chloro-3-indoyl-phosphate (Roche) for color reaction for 2 h or overnight at 4°C. Embryos were then rinsed with water and dehydrated in a graded ethanol series, then cleared in benzyl benzoate:benzyl alcohol (3:2) for observation.

Sectioning and microscopy

For more detailed analyses, selected embryos were sectioned before microscopic examination. For this purpose, embryos having undergone a long in situ coloration reaction were dehydrated and embedded in an epoxide resin (Poly/Bed 812, Polysciences, Warrington, PA, USA) according to the manufacturer's instructions. Embedded embryos were sectioned at 3–5-µm thickness (MT2-B Ultramicrotome, Sorvall, Ramsey, MN, USA) and mounted on glass slides using Permount (Fisher Scientific, Houston, TX, USA). Intact, or sectioned embryos were examined and photographed under DIC optics (Zeiss Axiophot [Zeiss, San Leandro, CA, USA] and Nikon Coolpix camera [Tokyo, Japan] or Nikon E800 [Technical Instruments, Burlingame, VT, USA] and Princeton Instruments cooled CCD camera [Roper Scientific, Tucson, AZ, USA] controlled by UIC Metamorph software). Images were processed, montaged and composed digitally (Metamorph, UIC; Photoshop, Adobe).

RESULTS

Partial cloning of *Hro-notch*

PCR using degenerate primers on a cDNA library made commercially from stage 7 to 10 *H. robusta* embryos (Stratagene) yielded an initial fragment of *Hro-notch*, which was expanded to 660 bp by 3′ RACE. This fragment encompassed part of the gene encoding an ankyrin repeat region and some sequence N-terminal to it. A 180-bp part of this fragment was used as probe to screen a λ DASHII genomic library made from *H. robusta* (Soto et al. 1997). Approximately 180,000 plaques were screened and eight independent clones were obtained. The entire insert in one of the clones, N4A1, was sequenced; it contained the portion of the putative *Hro-notch* gene encoding the entire intracellular domain (HRO-NICD). From this genomic sequence, primers were designed and used to amplify the *Hro-nicd* from first strand cDNA (see Materials and Methods). Alignment of conceptually translated HRO-NICD with those from other organisms shows that HRO-NICD is significantly smaller (Fig. 2), but nonetheless contains all domains characteristic for the NICD, viz. a nuclear localization domain, the ankyrin repeat region and a PEST domain. Comparison of the cDNA sequence with the genomic sequence revealed the presence of eight introns ranging in size from 95 to 156 bp. Furthermore, the 3′ UTR of the gene contains a putative cytoplasmic polyadenylation element (CPE) in addition to a polyadenylation sequence.

Hro-notch expression: semi-quantitative RT-PCR

Semiquantitative RT-PCR (Spencer and Christensen 1999) was used to estimate the relative levels of *Hro-notch* mRNA at selected stages of development. To control for variations in efficiency of RNA extraction and cDNA synthesis, sub maximal PCR amplification of 18S rRNA fragments was carried out in parallel for each sample. The primers were chosen to span introns in *Hro-notch*, so that PCR fragments arising from genomic DNA contamination could be distinguished by their larger size.

As found by this assay, *Hro-notch* was inherited maternally and was present at relatively low levels throughout cleavage (developmental stages 1–7; 0–29 h AZD) and during the period when teloblasts were producing blast cells (stages 5–8; approximately 15–80 h AZD; Fig. 3). Semi-quantitative RT-PCR also indicates that *Hro-notch* levels increased dramatically during the period of development coinciding with segmentation and organogenesis during stages 7–10 (approximately 40–160 h AZD).

In situ hybridization was used to obtain a more detailed description of *Hro-notch* expression and localization patterns, focusing primarily on developmental stages 7 and early 8 (29–69 h AZD), by which time all teloblasts have been born and are producing primary blast cells. *Hro-notch* mRNA was seen in both the teloblasts and the blast cells, as well as in the micromere derivatives that contribute cells to definitive nonsegmental structures and to the epibolizing epithelium.
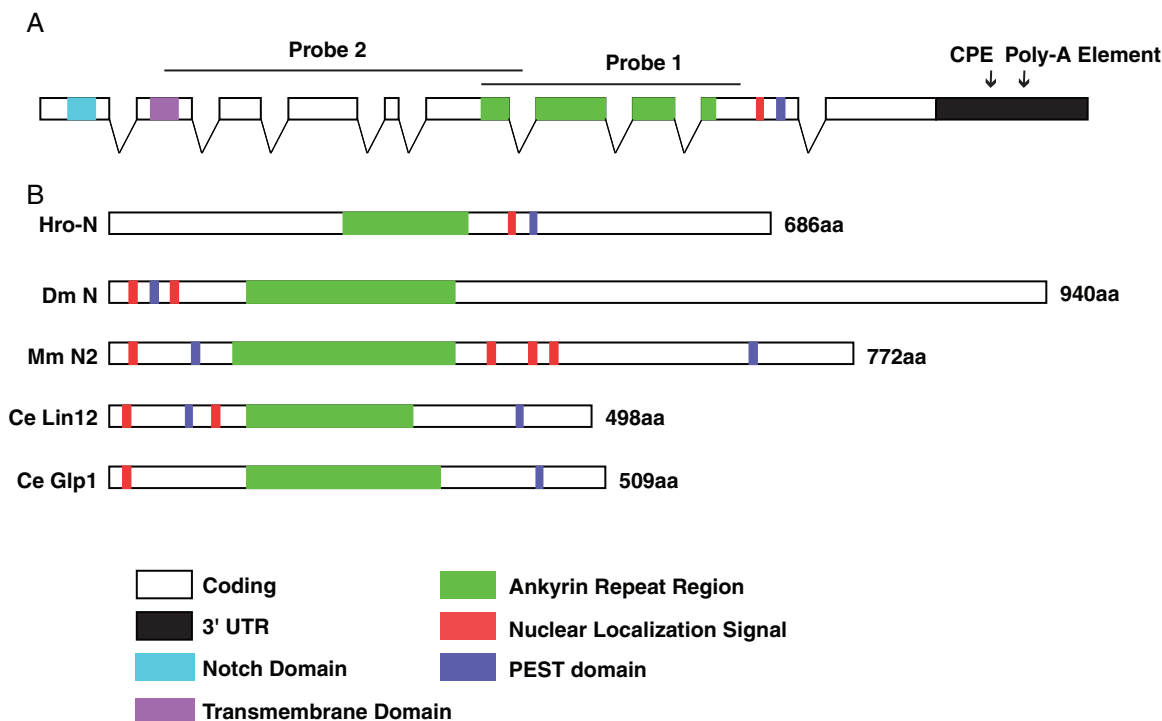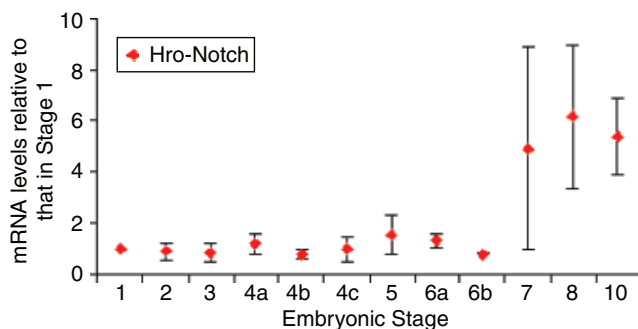
Fig. 2. *Hro-notch*, a *Notch* homolog in *Helobdella robusta*. (A) The genomic clone N4A1 contains the carboxy terminal portion of *Hro-notch*, from just upstream of the transmembrane domain through the 3′ untranslated region (UTR) and includes eight introns. (B) Comparison of the intracellular domains from Notch class genes in *H. robusta* (Hro N), *Caenorhabditis elegans* (Ce Lin12 and Ce Glp1), *Drosophila melanogaster* (Dm N), and *Mus musculus* (Mm N2). The accession numbers of sequences used for analysis are as follows, Mm Ntc2: O35,516; Ce Glp1: P13,508; Ce Lin12: P14,585; Dme N: P07,207. Programs used for analysis of the leech sequence: PEST find analysis (⟨http://www.at.embnet.org/embnet/tools/bio/PESTfind/⟩ http://www.at.embnet.org/embnet/tools/bio/PESTfind/) and PSORT11 (⟨http://psort.nibb.ac.jp/⟩ http://psort.nibb.ac.jp/).

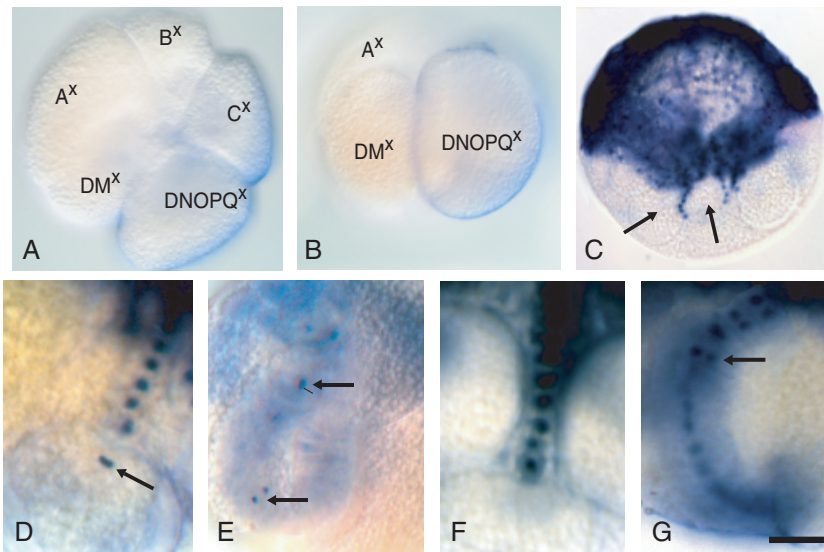## *Hro-notch* expression in proteloblasts and teloblasts

As described previously, teloblasts arise from the D quadrant, whose fate is determined by the segregation of teloplasm during the first three rounds of cleavage (Fig. 1). The unique D quadrant fate becomes manifest at fourth cleavage (9 h

Fig. 3. Expression of *Hro-notch*: semi-quantitative RT-PCR. In each experiment, the expression levels were plotted relative to stage 1. All other points represent the mean ± standard deviation of three separate experiments. See Materials and Methods for details.

AZD), when macromere D′ undergoes an obliquely equatorial division to generate proteloblasts DM and DNOPQ, precursors of mesoteloblasts and ectoteloblasts, respectively. In embryos fixed at this stage, *Hro-notch* expression was detected by in situ hybridization in DNOPQ, but not in DM (Fig. 4, A and B). *Hro-notch* transcripts appeared to be distributed uniformly in the cytoplasm of DNOPQ (Fig. 4, A and B), as in other early blastomeres that are positive for *Hro-notch* mRNA (F. C. G., unpublished).

Hro-notch transcripts were also present in the cytoplasm of all teloblasts by this criterion. But in about one-third of these cells (66 of 213 teloblasts scored in 37 embryos in six experiments), punctate spots of intense in situ staining were observed in addition to the diffuse cytoplasmic staining (Fig. 5). The reaction conditions that we found necessary to obtain meaningful in situ staining at the early stages of *Helobdella* development examined here were not compatible with double staining for DNA, so it was not possible to ascertain either the exact location of the chromatin or the mitotic phase of the teloblasts exhibiting the punctate staining. Given this limitation, prudence dictates that we use the phrase "punctate staining" to designate this aspect of the in situ pattern in teloblasts. Several

Fig. 4. Expression of *Hro-notch* in proteloblasts and bandlets: in situ hybridization. (A) Bright-field image of an embryo processed to reveal *Hro-notch* by in situ hybridization at stage 4. Blastomeres are labeled with superscript x to denote uncertainty regarding exactly when the embryo was fixed, and thus how many micromeres had been produced. (B) Lateral view of the embryo shown in (A). (C) Bright-field image of an embryo processed at early stage 8, showing more intense staining in the germinal bands and in ectodermal bandlets (arrows) that have not yet entered the germinal bands (cf. Fig. 1). The more intense staining correlates with the increase in overall *Hro-notch* levels at this stage, as judged by semi-quantitative RT-PCR. (D–G) Higher magnification views of embryos similar to that shown in (C), showing ectodermal (D and F) and mesodermal (E and G) bandlets in embryos subjected to shorter (D and E) or longer (F and G) coloration reactions (see text for details). Arrows indicate staining associated with the mitotic apparatus of a dividing ectoteloblast (D), primary mesodermal blast cells (lower arrow in E, G) and a secondary mesodermal blast cell (upper arrow in E). Scale bar, 100 µm in (A–C), 40 µm in (D and F), 50 µm in (E and G).
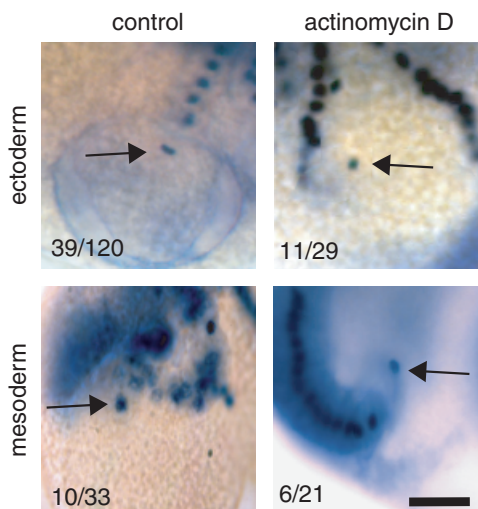
considerations led us to conclude that this punctate staining represents the association of *Hro-notch* transcripts with some part of the mitotic apparatus (defined as centrosomes, spindle, and chromatin) of teloblasts undergoing mitosis.

First, teloblasts are large cells, but much of the volume is occupied by yolk. The nucleus lies in a region of yolk-deficient cytoplasm adjacent to the column of descendant blast cells,

Fig. 5. Localization of *Hro-notch* transcripts to the mitotic apparatus in teloblasts is not sensitive to actinomycin-D. Representative images showing *Hro-notch* in situ staining associated with the presumptive mitotic apparatus (arrows) of meso- and ectoteloblasts in both control and actinomycin-D-treated embryos. Numbers indicate the proportion of teloblasts scored in which such punctate staining was observed. Scale bar, 40 µm.

and the punctate *Hro-notch* in situ stain was invariably in the region of the nucleus. Second, the proportion of teloblasts with punctate staining corresponds to the fraction of the teloblast cell cycle spent in mitosis (Bissen and Weisblat 1989). In sectioned material, we could not detect an intact nuclear envelope in teloblasts with punctate staining and we did not observe punctate staining in interphase teloblasts (as judged by the presence of an intact nuclear envelope; data not shown). Third, localization of developmental regulatory gene transcripts has been previously reported for lophotrochozoan species, including *eve-* and *hes*-class genes (to some component of the mitotic apparatus) in *H. robusta* (Song et al. 2002, 2004) and *eve-*, *dpp-*, and *tolloid*-class genes (to centrosomes) in *Ilyanassa obsoleta* (Lambert and Nagy 2002). These prior observations suggest that our present results are another example of an mRNA localization phenomenon that may be more prominent in *Lophotrochozoa*.

Assuming that these observations do indicate a cell-cycle dependent association of *Hro-notch* with the mitotic apparatus, several explanations seem likely. One is that *Hro-notch* is being transcribed during mitosis. The other is that pre-existing transcripts in the cytoplasm become associated with the mitotic apparatus during mitosis or some other part of the cell cycle. A third possibility is that for *Hro-notch* expression in teloblasts there is a cell cycle-dependent, differential regulation of the normally coupled processes of mRNA transcription, processing, and export or degradation.

To begin to distinguish between these possibilities, we treated embryos with transcription inhibitors, α-amanitin or actinomycin-D. Embryos treated with either inhibitor at concentrations sufficient to block the punctate staining of *Hro-hes*

in stage 7 embryos (Song et al. 2004) or *Hro-notch* transcription in two-cell embryos (F. C. G., unpublished) show the same patterns and frequency of cytoplasmic and punctate *Hro-notch* staining as untreated controls (Fig. 5). This suggests that the punctate staining does not result primarily from de novo transcription, but rather from cell cycle-dependent regulation of transcript localization and/or processing (Kondo et al. 2001).

Hro-notch expression in ectodermal blast cells

Each teloblast generates segmental founder cells (blast cells) in coherent columns (bandlets). During stages 7–8, bandlets merge ipsilaterally to form the germinal bands and thence, the germinal plate along the ventral mid-line of the embryo; segmental mesoderm and ectoderm differentiate in A–P progression within the germinal plate.

The strict birth order ranking of blast cells within each bandlet and the conserved patterns of cell division for each lineage make it possible to infer events within the primary blast cells (and their descendant clones) by comparing cells along the length of the bandlet (Zackson 1984; Bissen and Weisblat 1989). We used these features to analyze the dynamics of *Hro-notch* expression patterns in the mesodermal and ectodermal bandlets. Moreover, by adjusting the length of the final coloration reaction, we were able to distinguish qualitative and quantitative differences in the *Hro-notch* staining patterns in the mesodermal and ectodermal lineages.

Primary blast cells have dramatically prolonged cell cycles (approximately 10–28 h for the strain of *H. robusta* used here) relative to those of the parent teloblasts, most of which is spent in G2 phase (Bissen and Weisblat 1989). Ectodermal (n, o, p, and q) blast cells have not yet divided when they enter the germinal bands, but m blast cells divide when they are approximately 12 h old, that is, approximately 10 cells away from the parent M teloblast. The m blast cells divide with their spindles transverse to the A–P axis of the bandlet, so that the secondary blast cells lie side-by-side within the bandlet (Zackson 1984).

Inspection of embryos processed during stages 7–8 revealed that primary ectodermal blast cells that have not yet entered the germinal band stained intensely with a punctate pattern after even short reaction times (approximately 2 h at room temperature; Figs. 4 C, 4D, and 6A). The examination of sectioned embryos confirmed that this punctate staining pattern corresponded to the association of *Hro-notch* mRNA with interphase blast cell nuclei (Fig. 6C). Only after prolonged coloration reactions was cytoplasmic *Hro-notch* detected in the blast cells (Fig. 4F). Whether this nuclear staining represents active transcription or localization of *Hro-notch* mRNA will be addressed later.

In contrast to the situation in the isolated bandlets, blast cells within the germinal bands exhibited mainly diffuse cytoplasmic staining, with only occasional intense spots of punctate staining and some faint perinuclear staining (Fig. 6B); the micromere-derived epithelium overlying the germinal bands was largely devoid of *Hro-notch* transcripts (Fig. 6C). Ectodermal blast cells at the point of entry into the germinal band showed a transition from nuclear to perinuclear localization of transcripts (Fig. 6A). We conclude that the entry of ectodermal blast cells into the germinal band is associated with a dramatic change in the dynamics of *Hro-notch* transcription, transcript processing, and/or localization. As described above, ectodermal blast cells divide only after they have entered the germinal band. Although we were not able to combine lineage tracing and in situ hybridization to resolve the issue definitively, it seems likely that the punctate staining within the germinal bands corresponded to dividing ectodermal blast cells.

### *Hro-notch* expression in mesodermal blast cells

Under the reaction conditions that yielded intense punctate staining of interphase ectodermal blast cells, the cells in the mesodermal bandlet showed only faint cytoplasmic staining except for one or two punctately stained cells. These intensely stained cells lay at just the point in the mesodermal bandlet where the m blast cells undergo their side-by-side division (Fig. 4E). This cannot represent the same sort of nuclear staining seen in the interphase ectodermal blast cells because in these mitotic cells, the nuclei have presumably broken down.

In more intensely stained preparations (typically overnight at 4°C after several hours at room temperature), additional pairs of secondary mesodermal blast cells exhibited the same punctate pattern until the m blast cell clones entered the germinal bands. Under these prolonged coloration protocols, we also observed cytoplasmic and faintly punctate staining in primary m blast cells (Fig. 4G). Thus, our results suggest that *Hro-notch* levels are lower in primary mesodermal blast cells than in primary ectodermal blast cells, but that the subcellular distribution of the mRNA is similar in both lineages.

Transcription inhibitors do not eliminate nuclear localization of *Hro-notch* mRNA

The obvious interpretation of a nuclearly localized in situ signal is that it reflects relatively high level of transcriptional activity for the gene being studied. And if the nuclear signal is significantly higher than the cytoplasmic signal, it could be further supposed that transcription has just turned on in the cell, and/or that mRNA is rapidly being diluted or degraded.

In the experiments presented above, we found that the high nuclear/cytoplasmic ratio of the *Hro-notch* mRNA persisted essentially unchanged over many hours as seen by the consistent staining pattern of interphase blast cells along each bandlet. Therefore, the nuclear signal does not represent the
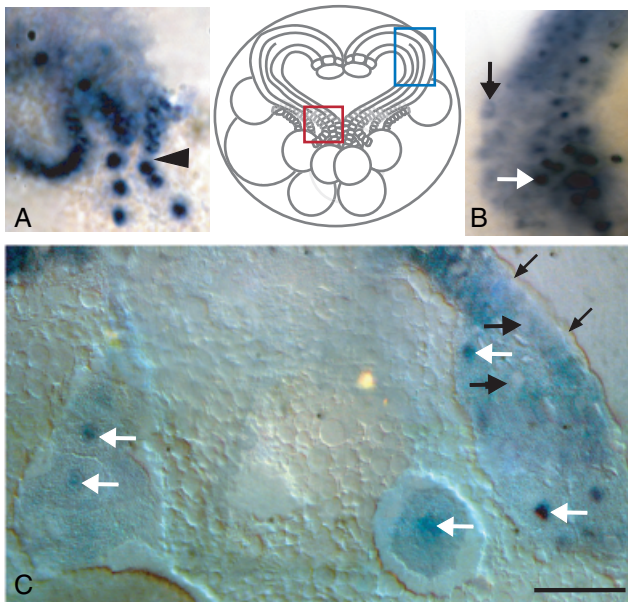
Fig. 6. *Hro-notch* localization changes as ectodermal blast cells enter the germinal bands. (A) A close-up view of an intact embryo processed for *Hro-notch* at early stage 8, focusing on the point where the ectodermal bandlets enter the germinal band (corresponding to the area boxed in red in the schematic). As in Fig. 4, staining in the primary ectodermal blast cells is punctate within the bandlets (solid staining below the arrowhead), but becomes perinuclear as the bandlets enter the germinal bands (hollow staining patterns above arrowhead). (B) Close-up view of a similar embryo, showing a portion of the germinal band (corresponding to the area boxed in blue in the schematic). Both punctate (white arrow) and presumptively perinuclear (black arrow) staining are seen. (C) DIC image showing part of a similar embryo, embedded and sectioned; punctate staining is seen in blast cells that have not yet entered the germinal bands (three leftmost white arrows) and in cells within the germinal band (two rightmost white arrows). At least four of these cells are in interphase, as judged by their intact nuclear envelopes. Cytoplasmic staining is seen within the germinal band and some blast cells exhibit perinuclear staining (large black arrows). Within the overlying micromere-derived epithelium (small black arrows) *Hro-notch* transcripts are not detected. Scale bar, 80 μm in (A), 60 μm in (B), 20 μm in (C).

initiation of *Hro-notch* transcription. Moreover, the blast cell nuclei occupy a significant fraction of the blast cell volume; thus, dilution of exported transcripts is unlikely to account for the persistently low cytoplasmic signal over so many hours.

It is thus likely that the patterns of *Hro-notch* transcript distribution observed in the blast cells represent active transcription combined with rapid degradation of cytoplasmic message, localization/retention of *Hro-notch* mRNA in the nucleus, or some combination of the two. To distinguish among these possibilities, we compared the *Hro-notch* in situ patterns of control embryos with siblings in which transcription had been inhibited by treatment with either actinomycin-D or α-amanitin. Previous work has shown that global in-

hibition of transcription in *Helobdella* slows the divisions of the teloblasts only slightly (so they continue to form blast cells), but does block the divisions of primary to secondary blast cells (Bissen and Weisblat 1991). We thus applied transcriptional inhibitors actinomycin-D and α-amanitin to stages 6 and 7 embryos and allowed them to continue blast cell divisions for up to 24 h. If the mRNA were being rapidly made and degraded, inhibiting transcription should have resulted in clearing of the in situ signal from the cells.

In sharp contrast to this prediction, the punctate staining persisted in blast cells (and also teloblasts, as discussed earlier) after transcription was inhibited. In fact, after 17–24 h of transcriptional inhibition, we observed no obvious effects on the *Hro-notch* staining pattern in the ectodermal lineages (Fig. 7A). Moreover, teloblasts fixed while undergoing cytokinesis have two distinct pools of punctate staining, corresponding to the parent teloblast and the nascent blast cell (Fig. 7B).

Transcription inhibitors did have a reproducible effect on the *Hro-notch* pattern in the mesodermal bandlet, however. The youngest m blast cells (i.e., proximal to the M teloblast within the m bandlet) were strongly stained; the next older cells show slightly less *Hro-notch* mRNA and this gradient of decreasing *Hro-notch* in situ signal continued along the length of the (undivided) primary blast cells. This pattern suggests that the blast cells inherited *Hro-notch* mRNA from a relatively stable store in the M teloblast, and that the inherited mRNA was then gradually degraded as the primary blast cells aged.

This interpretation is complicated by the observation that rather intense punctate staining was still seen associated with the most recently divided m blast cells in the inhibitor-treated embryos (Fig. 7). To investigate this further, we combined lineage tracer injection with transcription inhibitor treatments, and replicated results obtained previously with embryos of *H. triserialis* (Bissen and Weisblat 1991): after a treatment of 17–24 h with actinomycin-D or α-amanitin blast cell production continued, at a slightly slower rate than in controls; and the (tracer labeled) blast cells born after inhibitor treatment failed to divide. Interestingly however, the last blast cells born just before inhibitor treatment had divided or initiated division (Fig. 7), despite the fact that they were exposed to the inhibitor for essentially the same time as the first cells produced during the treatment. The daughter cells arising from m blast cells that had undergone mitosis in the presence of transcription inhibitor remained rounded up with small-condensed nuclei, suggesting that they had arrested in telophase. In these cells, *Hro-notch* staining appeared as small dark spots (Fig. 7). These results suggest that even after many hours in transcription inhibitors, blast cells still retained some *Hro-notch* transcripts and were capable of relocalizing them to the mitotic apparatus. They also indicate that in embryos treated with transcription inhibitors α-amanitin or actinomycin-D, blast cells retained the ability to initiate
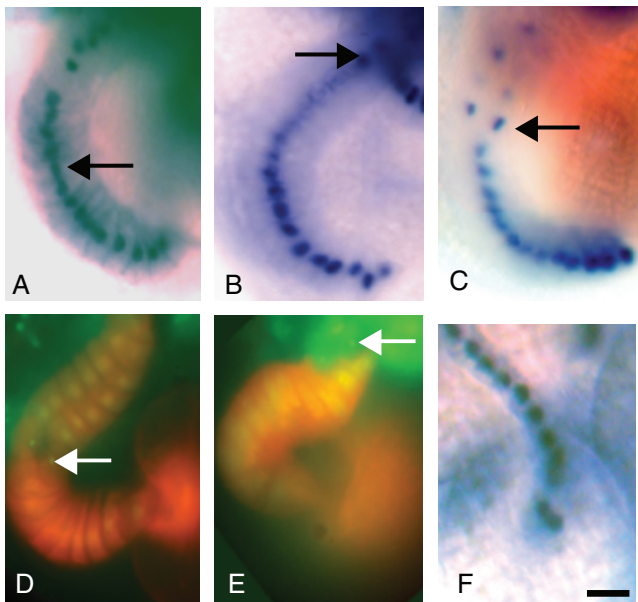
Fig. 7. Differences in α-amanitin-sensitivity of *Hro-notch* expression in mesodermal and ectodermal bandlets. In (A–C) and (F), in situ hybridization with long coloration reactions were used to visualize *Hro-notch* transcripts. (A–C) Mesodermal (m) bandlets in embryos fixed 17–24 h after injection with water (A) or α-amanitin (B and C). Embryos are oriented so as to keep the curved bandlets in one plane, which sometimes obscures the point of first mitosis (arrows). Note that in the embryos injected with alpha-amanitin (B and C), the number of undivided primary blast cells is greater than in the water-injected control (A). (D and E) Embryos co-injected with lineage tracer and water (D) or α-amanitin (E), then fixed and counterstained with Sytox green after 19 h of further development. In the control embryo (D) there are nine undivided primary m blast cells and at least 7 m blast cell clones that have already initiated divisions. In the α-amanitin-injected embryo (E), none of the primary blast cells produced as the injection have divided. The last cell born before injection appears to have arrested in mitosis, showing two cells with punctate chromatin (arrow). (F) An ectodermal bandlet from the batch of embryos shown in (A–C) shows no obvious difference from ectodermal bandlets in control embryo (see Fig. 4F). Scale bar, 50 μm in (A–E), 40 μm in (F).

(although not necessarily complete) division as long as they were born before the inhibitor treatment.

CONCLUSIONS

Overview

In the embryonic development of clitellate annelids such as the leech *H. robusta*, segments arise from parallel arrays of segmental founder cells (blast cells) produced from a clearly defined posterior growth zone comprising five bilateral pairs of identified and experimentally accessible stem cells (teloblasts). Thus, the 10 teloblasts constitute an almost idealized example of a posterior growth zone. Teloblastic segmentation also occurs in some crustacean arthropods (Anderson 1973)

but segmentation in leech differs from that in arthropods in two significant ways. First, the clones of individual blast cells interdigitate extensively along the A–P axis (Weisblat and Shankland 1985), so there is nothing analogous to the process that restricts cell mingling to within subsegmental compartments in the embryos of *Drosophila* and other arthropods (Dohle and Scholtz 1997). Second, from each N and Q lineage, two blast cells are required to make one segment's worth of progeny; these two blast cells in each N and Q lineage undergo distinct patterns of cell divisions and contribute distinct patterns of definitive progeny. Thus, the N and Q teloblasts undergo a grandparental mode of stem cell divisions, in contrast to the parental mode of the crustacean teloblasts (and the M and O/P teloblasts in leech) (reviewed in Scholtz 2002).

The extent to which this teloblastic mode of segmentation operates even in nonclitellate annelids (reviewed in Seaver 2003) remains to be elucidated, as do the evolutionary relationships (convergent vs. plesiomorphic) of the segmentation processes seen in annelids, arthropods, and vertebrates. It will be argued below that resolution of these questions will require detailed descriptive and mechanistic studies of segmentation in diverse taxa at both the cellular and molecular levels. Toward that end, we have previously reported that *even-skipped*- and *hes*-related genes are expressed in the teloblasts and blast cells of *H. robusta* embryos (Song et al. 2002, 2004). Notch signaling activates *hes* expression in many developmental contexts, including vertebrate somitogenesis and apparently spider segmentation (Stollewerk et al. 2003). Here we have begun to examine the expression of *Hro-notch*.

Dynamic expression and localization of *Hro-notch* transcripts in teloblasts and blast cells

During teloblast formation, *Hro-notch* is expressed preferentially in the ectodermal precursor cell DNOPQ (2d in classical spiralian nomenclature) but was not detected in the mesodermal precursor DM (2D). Following cleavage, *Hro-notch* transcripts are present in both mesodermal and ectodermal teloblasts and blast cells, but remain at higher levels in ectodermal lineages as judged by the intensity of the in situ hybridization signal.

Hro-notch transcripts localize to the mitotic apparatus of dividing m blast cells and are apparently localized to the mitotic apparatus of dividing teloblasts as well. In *Xenopus*, localization of *Xbub3* and *cyclinB1* transcripts to the mitotic apparatus is mediated in part by CPEs in the 3′ UTR (Groisman et al. 2000). In *Ilyanassa*, transcripts of *even-skipped*, *decapentaplegic*, and *tolloid* homologs localize to the pericentriolar matrix of certain blastomeres (Lambert and Nagy 2002), but the 3′ UTR sequence of those transcripts was not obtained. In *Helobdella*, we have previously reported the localization of *even-skipped* and *hes* homologs to the mitotic

apparatus of dividing teloblasts and blast cells and find CPEs in the 3′ UTRs of those transcripts (Song et al. 2002, 2004), as we do for *Hro-notch*. In contrast to our results with *Hro-hes*, however, we find no evidence that *Hro-notch* is transcribed during mitosis; transcription inhibitors do not abrogate the punctate staining seen in mitotic cells.

Another noteworthy aspect of the *Hro-notch* transcript distribution is their nuclear localization in interphase blast cells, especially in the ectodermal lineages. The fact that this staining is also resistant to treatment with transcription inhibitors suggests that it does not reflect robust transcription or rapid turnover so much as the distribution and stability of transcripts inherited from the parent teloblasts, which we call "teloternal" transcripts. Teloternal transcripts are also observed in the M lineage, but at lower levels. Moreover, these mesodermal *Hro-notch* transcripts are more rapidly degraded, as judged by the clearing of in situ signal from older primary blast cells upon treatment with transcription inhibitors.

Canonical Notch signaling is regulated by ligand-dependent cleavage of the transmembrane domain to release the NICD (Selkoe and Kopan 2003). But in leech, the fates of blast cells show little dependence on specific cell–cell signaling (Bissen and Weisblat 1987; Nardelli-Haefliger and Shankland 1992; Gleizer and Stent 1993; Seaver and Shankland 2001). Understanding the full significance of the *Hro-notch* expression patterns must await a similarly detailed analysis of the dynamics of HRO-NOTCH protein expression. Pending this, we speculate that the localization or retention of *Hro-notch* in the nucleus of interphase cells in the bandlets of primary blast cells could reflect another mechanism for regulating Notch signaling. Once the ectodermal bandlets coalesce, *Hro-notch* transcripts become more diffusely cytoplasmic, but with a strong perinuclear component that could reflect docking at the rough endoplasmic reticulum as part of translational activation. This position-dependent transition in localization suggests that cell–cell signaling plays a role in the localization of *Hro-notch* transcripts.

In the mesodermal blast cells, *Hro-hes* transcription turns on before the bandlets coalesce, as indicated by the sensitivity of the in situ signal to treatment with transcription inhibitors. *Hro-notch* shows a higher proportion of cytoplasmic to nuclear signal in mesodermal blast cells than in the ectoderm. But when m blast cells divide, the cytoplasmic *Hro-notch* is stably localized to the mitotic apparatus. Thus, *Hro-notch* localization appears to be regulated in both a cell cycle and cell contact-dependant manner.

Comparisons with other animals

Within each of the three main clades of eusegmented animals (annelids, arthropods, and vertebrates), processes of segmentation resemble one another in that the basal condition seems to be the sequential formation of trunk segments from a pos-

terior zone of growth or differentiation (Balavoine and Adoutte 2003). Recently, intriguing molecular similarities have been discovered between segmentation mechanisms in organisms considered to have arisen from basal branches of the arthropod lineage and those in vertebrates, where involvement of a biochemical oscillator involving Notch/Hes signaling is now well-documented (reviewed by Pourquie 2001).

For example, in the spider *C. salei*, expression of a *hairy* homolog appears to oscillate in the presegmental tissues (Damen et al. 2000) and anti-sense disruption of Notch signaling disrupts the formation of normal segmental boundaries (Stollewerk et al. 2003). Similarly, in the centipede *Lithobius forficatus*, dynamic expression of a *delta* homolog also suggests involvement of the Notch pathway in segmentation (Kadner and Stollewerk 2004). Accordingly, it has been suggested that the ancestral arthropod had a Notch signaling-dependent segmentation clock with some pair rule genes (i.e., *hairy*, *runt*, and *eve* homologs) being patterned by the clock, and/or functioning within the clock (Peel 2004).

With our present and previous work, it now appears that homologs of *eve*, *hes*, and *notch* are also expressed and/or localized in an oscillatory (cell cycle-dependent) manner in the teloblastic growth zone of the leech, representing the third clade of eusegmented animals. It may be argued that this data, especially taken with the expression patterns of segmentation gene homologs in *Platynereis* (de Rosa et al. 2005), is evidence that the last common ancestor of annelids, arthropods, and vertebrates was already segmented. In our view, several factors preclude drawing a firm conclusion on this topic.

First, the "usual suspects" in which segmentation mechanisms are commonly compared are not the only groups that show metamerism. The body plans of taxa such as flatworms, molluscs, pogonophorans, and kinorhynchs all exhibit "grades" of segmentation, in which metamerism of neural or other organ system are seen, and studies on the eusegmented taxa should be interpreted in the context of these other taxa. The existence of taxa with grades of segmentation has been used to argue variously in favor of (1) a segmented ancestor of all Bilateria with multiple losses of segmented tissues in various descendents (Balavoine and Adoutte 2003), (2) a single segmented ancestor of the annelids and arthropods (Scholtz 2002) to the exclusion of other groups, or (3) a continuum of grades of segmentation in general (Budd 2001). However, without knowing their phylogenetic relationships, how can we distinguish between the possibilities that the various metameric taxa reflect ancestral intermediates in the evolution of segmentation, loss of ancestral segmentation, or multiple independent acquisitions of metamerism?

Second, it could be argued that, as the number of cellular signaling pathways is limited and Notch signaling is involved in so many developmental processes (at least in vertebrates and *Drosophila*), it would be more surprising if it was not used

in segmentation. In addition to Notch, recent work has indicated that two of the other canonical signaling pathways, Wnt and FGF, are also involved in somitogenesis (Aulehla et al. 2003; Dubrulle and Pourquie 2004). It is intriguing that Notch and/or Wnt signaling are also involved in vertebrate stem cell processes including haematopoiesis, osteogenesis, neurogenesis, and gut formation (Baker 2000; Bonde et al. 2004; Lee and Kaestner 2004; Nuttall and Gimble 2004). We have previously suggested a "stem cell model" according to which segmentation could have evolved independently in various taxa by modification of the inherent periodicity of stem cell division and cell fate decisions present in an unsegmented ancestor (Song et al. 2004). Our present findings of oscillation in *Hro-notch* localization are also consistent with this hypothesis.

Finally, it is sometimes argued that one animal or another is more informative for evo-devo studies because of its "basal" phylogenetic position, presumably under the assumption that (shades of Haeckel?) species with morphologically derived adults must feature equally derived processes throughout development. We must bear in mind, however, that all extant animals are by definition "modern" and there is growing evidence of remarkable flexibility in what is conserved and what varies during evolution—structures or operational processes can be highly conserved despite dramatic changes in the underlying molecular mechanisms by which they are achieved. The homology of segmentation among arthropods is unquestioned, for example, and yet there is a broad range of both cellular and molecular patterning processes. Given this flexibility, one can envision a scenario in which: (1) morphological segmentation arose independently in various bilaterian lineages using various signaling pathways and then (2) during subsequent evolution, the Notch/Hes pathway was recruited to become part of the cell/biochemical oscillator by which the repeating units were formed.

Future directions

Despite the current level of ambiguity, we are optimistic that the evolution of segmentation can eventually be resolved. At the heart of the matter is the need for further work in animal phylogeny and experimental embryology. For example, as discussed above, improving the resolution of the phylogenetic tree is essential for evaluating the competing interpretations of the significance of the metameric taxa.

Improved knowledge of phylogenetic relationships will also be helpful for interpreting the results of comparative embryological investigations. Likewise, much more experimental work is required to remedy the lack of mechanistic information regarding A–P patterning in animals other than *Drosophila* and vertebrates. What is the developmental significance of the arthropod-like expression patterns of *engrailed-* and *wnt*-related genes in *Platynereis* (Prud'homme

et al. 2003) or the cell cycle-dependent expression of *notch-*, *eve-*, and *hes*-related genes in *Helobdella*? How do metameric or segmental patterns arising in flatworms, molluscs, and onychophorans relate to the segmentation in annelids and arthropods?

Much work on "nonmodel" organisms remains to be performed before we can draw firm conclusions about the evolutionary origins of segmentation. But thanks to the previous insights obtained largely from *Drosophila* and vertebrates, there is a useful set of experimental and conceptual tools that can be applied. The phylogenetic position and experimental tractability of the *Helobdella* embryo make it a useful object for future work.

REFERENCES

Aguinaldo, A. M., et al. 1997. Evidence for a clade of nematodes, arthropods and other moulting animals. *Nature* 387: 489–493.

Anderson, D. 1973. *Embryology and Phylogeny in Annelids and Arthropods.* Pergamon Press, Oxford.

Aulehla, A., et al. 2003. Wnt3a plays a major role in the segmentation clock controlling somitogenesis. *Dev. Cell* 4: 395–406.

Baker, N. E. 2000. Notch signaling in the nervous system. Pieces still missing from the puzzle. *Bioessays* 22: 264–273.

Balavoine, G., and Adoutte, A. 2003. The segmented Urbilateria: a testable scenario. *Integr. Comp. Biol.* 43: 137–147.

Bissen, S., and Weisblat, D. 1989. The duration and composition of cell cycles in leech, *Helobdella robusta. Development* 106: 105–118.

Bissen, S. T., and Weisblat, D. A. 1987. Early differences between alternate n blast cells in leech embryo. *J. Neurobiol.* 18: 251–269.

Bissen, S. T., and Weisblat, D. A. 1991. Transcription in leech: mRNA synthesis is required for early cleavages in *Helobdella* embryos. *Dev. Biol.* 146: 12–23.

Blair, S. T., and Weisblat, D. A. 1984. Cell interactions in the developing epidermis of the leech *Helobdella triserialis. Dev. Biol.* 101: 318–325.

Bonde, J., Hess, D. A., and Nolta, J. A. 2004. Recent advances in hematopoietic stem cell biology. *Curr. Opin. Hematol.* 11: 392–398.

Braun, J., and Stent, G. S. 1989. Axon outgrowth along segmental nerves in the leech: I. Identification of candidate guidance cells. *Dev. Biol.* 132: 471–485.

Budd, G. E. 2001. Why are arthropods segmented? *Evol. Dev.* 3: 332–342.

Cooke, J., and Zeeman, E. C. 1976. A clock and wavefront model for control of the number of repeated structures during animal morphogenesis. *J. Theor. Biol.* 58: 455–476.

Damen, W. G., Weller, M., and Tautz, D. 2000. Expression patterns of hairy, even-skipped, and runt in the spider *Cupiennius salei* imply that these genes were segmentation genes in a basal arthropod. *Proc. Natl. Acad. Sci. USA* 97: 4515–4519.

Davis, G. K., and Patel, N. H. 1999. The origin and evolution of segmentation. *Trends Cell Biol.* 9: M68–M72.

de Rosa, R., Prud' homme, B., and Balavoine, G. 2005. Caudal and even-skipped in the annelid *Platynereis dumerilii* and the ancestry of posterior growth. *Evol. Dev.* 7: 574–587.

Dohle, W., and Scholtz, G. 1997. How far does cell lineage influence cell fate specification in crustacean embryos? *Semin. Cell Dev. Biol.* 8: 379–390.

Dubrulle, J., and Pourquie, O. 2004. Fgf8 mRNA decay establishes a gradient that couples axial elongation to patterning in the vertebrate embryo. *Nature* 427: 419–422.

Evrard, Y. A., Lun, Y., Aulehla, A., Gan, L., and Johnson, R. L. 1998. Lunatic fringe is an essential mediator of somite segmentation and patterning. *Nature* 394: 377–381.

Fernandez, J. 1980. Embryonic development of the glossiphoniid leech *Theromyzon rude*: characterization of developmental stages. *Dev. Biol.* 76: 245–262.

Gleizer, L., and Stent, G. S. 1993. Developmental origin of segmental identity in the leech mesoderm. *Development* 117: 177–189.

Goto, A., Kitamura, K., Arai, A., and Shimizu, T. 1999. Cell fate analysis of teloblasts in the Tubifex embryo by intracellular injection of HRP. *Dev. Growth Differ.* 41: 703–713.

Groisman, I., Huang, Y. S., Mendez, R., Cao, Q., Theurkauf, W., and Richter, J. D. 2000. CPEB, maskin, and cyclin B1 mRNA at the mitotic apparatus: implications for local translational control of cell division. *Cell* 103: 435–447.

Holmgren, R. 1984. Cloning sequences from the hairy gene of *Drosophila*. *EMBO J* 3: 569–573.

Huang, F. Z., Bely, A. E., and Weisblat, D. A. 2001. Stochastic WNT signaling between nonequivalent cells regulates adhesion but not fate in the two-cell leech embryo. *Curr. Biol.* 11: 1–7.

Kadner, D., and Stollewerk, A. 2004. Neurogenesis in the chilopod *Lithobius forficatus* suggests more similarities to chelicerates than to insects. *Dev. Genes Evol.* 214: 367–379.

Kimmel, C. B. 1996. Was Urbilateria segmented? *Trends Genet.* 12: 329–331.

Kondo, T., Kotani, T., and Yamashita, M. 2001. Dispersion of cyclin B mRNA is coupled with translational actication of the mRNA during zebrafish oocyte maturation. *Dev. Biol.* 229: 421–431.

Lambert, J. D., and Nagy, L. M. 2002. Asymmetric inheritance of centrosomally localized mRNAs during embryonic cleavages. *Nature* 420: 682–686.

Lee, C. S., and Kaestner, K. H. 2004. Clinical endocrinology and metabolism. Development of gut endocrine cells. *Best Pract. Res. Clin. Endocrinol. Metab.* 18: 453–462.

Lewis, J. 2003. Autoinhibition with transcriptional delay: a simple mechanism for the zebrafish somitogenesis oscillator. *Curr. Biol.* 13: 1398–1408.

Morales, A. V., Yasuda, Y., and Ish-Horowicz, D. 2002. Periodic Lunatic fringe expression is controlled during segmentation by a cyclic transcriptional enhancer responsive to notch signaling. *Dev. Cell* 3: 63–74.

Muller, M., Weizsacker, E., and Campos-Ortega, J. A. 1996. Expression domains of a zebrafish homologue of the *Drosophila* pair-rule gene hairy correspond to primordia of alternating somites. *Development* 122: 2071–2078.

Nardelli-Haefliger, D., and Shankland, M. 1992. Lox2, a putative leech segment identity gene, is expressed in the same segmental domain in different stem cell lineages. *Development* 116: 697–710.

Nuttall, M. E., and Gimble, J. M. 2004. Controlling the balance between osteoblastogenesis and adipogenesis and the consequent therapeutic implications. *Curr. Opin. Pharmacol.* 4: 290–294.

Palmeirim, I., Henrique, D., Ish-Horowicz, D., and Pourquie, O. 1997. Avian hairy gene expression identifies a molecular clock linked to vertebrate segmentation and somitogenesis. *Cell* 91: 639–648.

Peel, A. 2004. The evolution of arthropod segmentation mechanisms. *Bioessays* 26: 1108–1116.

Pourquie, O. 2001. The vertebrate segmentation clock. *J. Anat.* 199: 169–175.

Prud'homme, B., et al. 2003. Arthropod-like expression patterns of engrailed and wingless in the annelid *Platynereis dumerilii* suggest a role in segment formation. *Curr. Biol.* 13: 1876–1881.

Scholtz, G. 2002. The Articulata Hypothesis—or what is a segment? *Organisms Div. Evol.* 2: 197–215.

Schoppmeier, M., and Damen, W. G. 2005. Suppressor of Hairless and Presenilin phenotypes imply involvement of canonical Notch-signalling in segmentation of the spider *Cupiennius salei*. *Dev. Biol.* 280: 211–224.

Seaver, E. C. 2003. Segmentation: mono- or polyphyletic? *Int. J. Dev. Biol.* 47: 583–595.

Seaver, E. C., and Shankland, M. 2001. Establishment of segment polarity in the ectoderm of the leech *Helobdella*. *Development* 128: 1629–1641.

Selkoe, D., and Kopan, R. 2003. Notch and Presenilin: regulated intramembrane proteolysis links development and degeneration. *Annu. Rev. Neurosci.* 26: 565–597.

Shankland, M., Bissen, S. T., and Weisblat, D. A. 1992. Description of the Californian leech *Helobdella robusta* sp. nov., comparison with *Helobdella triserialis* on the basis of morphology, embryology, and experimental breeding. *Can. J. Zool.* 70: 1258–1263.

Song, M. H., Huang, F. Z., Chang, G. Y., and Weisblat, D. A. 2002. Expression and function of an even-skipped homolog in the leech *Helobdella robusta*. *Development* 129: 3681–3692.

Song, M. H., Huang, F. Z., Gonsalves, F. C., and Weisblat, D. A. 2004. Cell cycle-dependent expression of a hairy and Enhancer of split hes homolog during cleavage and segmentation in leech embryos. *Dev. Biol.* 269: 183–195.

Soto, J. G., Nelson, B. H., and Weisblat, D. A. 1997. A leech homolog of twist: evidence for its inheritance as a maternal mRNA. *Gene* 199: 31–37.

Spencer, W. E., and Christensen, M. J. 1999. Multiplex relative RT-PCR method for verification of differential gene expression. *Biotechniques* 27: 1044–1046, 1048–1050, 1052.

Stollewerk, A., Schoppmeier, M., and Damen, W. G. 2003. Involvement of Notch and Delta genes in spider segmentation. *Nature* 423: 863–865.

Weisblat, D. A., and Shankland, M. 1985. Cell lineage and segmentation in the leech. *Philos. Trans. R. Soc. London B Biol. Sci.* 312: 39–56.

Willmer, P. 1990. *Invertebrate Relationships: Patterns in Animal Evolution*. Cambridge University Press, Cambridge.

Zackson, S. L. 1984. Cell lineage, cell–cell interaction, and segment formation in the ectoderm of a glossiphoniid leech embryo. *Dev Biol* 104: 143–160.

Zhang, S. O., and Weisblat, D. A. 2005. Applications of mRNA injections for analyzing cell lineage and asymmetric cell divisions during segmentation in the leech *Helobdella robusta*. *Development* 132: 2103–2113.